JACS
JOURNAL OF THE AMERICAN CHEMICAL SOCIETY
Article
pubs.acs.org/JACS
Terms of Use

Symmetrized Photoinitiated Electron Flow within the [Myoglobin:Cytochrome b_5] Complex on Singlet and Triplet Time Scales: Energetics vs Dynamics

Nadia Petlakh Co,[†] Ryan M. Young,[†,‡] Amanda L. Smeigh,[†,‡] Michael R. Wasielewski,[†,‡] and Brian M. Hoffman*[,†]

[†]Department of Chemistry and [‡]Argonne-Northwestern Solar Energy Research (ANSER) Center, Northwestern University, Evanston, Illinois 60208-3113, United States

Supporting Information

ABSTRACT: We report here that photoinitiated electron flow involving a metal-substituted (M = Mg, Zn) myoglobin (Mb) and its physiological partner protein, cytochrome b_5 (cyt b_5) can be "symmetrized": the [Mb:cyt b_5] complex stabilized by three D/E → K mutations on Mb (D44K/D60K/E85K, denoted MMb) exhibits both oxidative and reductive ET quenching of both the singlet and triplet photoexcited MMb states, the direction of flow being determined by the oxidation state of the cyt b_5 partner. The first-excited singlet state of MMb (^{1}MMb) undergoes ns-time scale reductive ET quenching by Fe^{2+}cyt b_5 as well as ns-time scale oxidative ET quenching by Fe^{3+}cyt b_5, both processes involving an ensemble of structures that do not interconvert on this time scale. Despite a large disparity in driving force favoring photooxidation of ^{1}MMb relative to photoreduction ($\delta(-\Delta G^0) \approx 0.4$ eV, M = Mg; ≈ 0.2 eV, M = Zn), for each M the average rate constants for the two reactions are the same within error, $^1k_f > 10^8$ s^{-1}. This surprising observation is explained by considering the driving-force dependence of the Franck−Condon factor in the Marcus equation. The triplet state of the myoglobin (^{3}MMb) created by intersystem crossing from ^{1}MMb likewise undergoes reductive ET quenching by Fe^{2+}cyt b_5 as well as oxidative ET quenching by Fe^{3+}cyt b_5. As with singlet ET, the rate constants for oxidative ET quenching and reductive ET quenching on the triplet time scale are the same within error, $^3k_f \approx 10^5$ s^{-1}, but here the equivalence is attributable to gating by intracomplex conversion among a conformational ensemble.

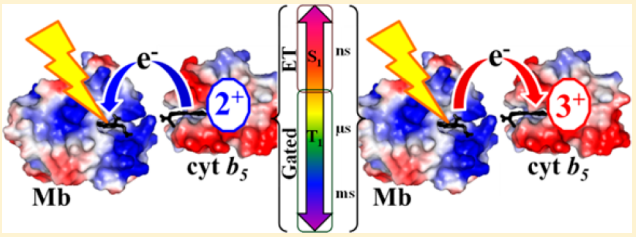

INTRODUCTION

Cytochrome b_5 (cyt b_5) reacts with myoglobin (Mb) as part of a physiological repair system in which autooxidized and inactive Fe^{3+}Mb is reduced to its active Fe^{2+}Mb O_2-storage form by electron transfer (ET) from Fe^{2+}cyt b_5.[1,2] The [Mb:cyt b_5] complex has served as a paradigm for interprotein ET between dynamically docked partners whose binding and reactivity are decoupled; many conformations of the complex contribute to binding but few to ET.[3] In recent years, we have demonstrated that binding and reactivity can be enhanced and coupled in the [Mb:cyt b_5] complex through mutations on the MbWT surface and/or heme neutralization. These generate a suite of positively charged Mb's whose binding to the negatively charged b_5 increases with the charge product of the proteins ($-q_{Mb}q_{cyt\ b5}$);[4,5] ET between the Mb's and cyt b_5 was probed through replacement of the heme group in Mb with a porphyrin containing a closed-shell metal ion (Zn^{2+}), with the focus being photooxidation of the photoexcited triplet state, ^{3}ZnMb. Most of this work studied ^{3}ZnMb by Fe^{3+}cyt b_5 on the time scale of milliseconds−seconds. However, photoexcitation of ZnMb directly populates the first-excited singlet state, S_1, and we discovered interprotein photooxidative singlet ET within a redesigned [ZnMb:cyt b_5] complex at rate constants that approach those occurring within the photosynthetic reaction centers, $k_{ET} = 2.1 \times 10^9$ s^{-1}.[6]

In the rich history of photoinitiated interprotein ET where one partner is a metal-substituted hemoprotein (M = H_2 as well as Mg, Zn), the exclusive focus has been on oxidative ET quenching of the photoexcited protein partner,[7−15] despite the fact that photoreduction of M-porphyrins is energetically favorable,[16,17] and that there have been reports of reductive and oxidative quenching of photoexcited Zn-substituted proteins by small molecules.[18,19] We report here that photoinitiated electron flow involving a metal-substituted hemoprotein and its physiological partner protein can indeed be "symmetrized": the [Mb:cyt b_5] complex stabilized by three D/E → K mutations on Mb (MMb(D44K/D60K/E85K), denoted MMb; M = Mg or Zn) exhibits *both* oxidative and reductive ET quenching of *both* the singlet and triplet photoexcited MMb states, the direction of flow being determined by the oxidation state of the cyt b_5 partner. We find that the first-excited singlet state, S_1, of the Mb-incorporated metalloporphyrin, denoted ^{1}MMb, undergoes nanosecond-time scale reductive ET

Received: June 25, 2014
Published: August 18, 2014

   dx.doi.org/10.1021/ja506388c | J. Am. Chem. Soc. 2014, 136, 12730−12736

quenching in which an electron is transferred *to* ^{1}MMb from Fe^{2+}cyt b_5, as well as nanosecond-time scale oxidative ET quenching in which an electron is transferred *from* ^{1}MMb to Fe^{3+}cyt b_5. Surprisingly, the rate constants for the two intracomplex reactions are the same within error, with average rate constants, $^1k_f \approx 10^8$ s^{-1}, a phenomenon that is explainable on energetic grounds. The progress curves in both cases are nonexponential and viscosity independent, implying the presence of ensembles of structures that do not interconvert on the time scale of the measurement.

The triplet state of the mutant, ^{3}MMb, created by intersystem crossing (ISC) from ^{1}MMb likewise undergoes reductive ET quenching by the Fe^{2+}cyt b_5 as well as oxidative ET quenching by the Fe^{3+}cyt b_5. Again, surprisingly, the rate constants for the two intracomplex reactions are the same within error, $^3k_f \approx 10^5$ s^{-1}, despite a large disparity in driving forces. However, in this case the shape and viscosity dependence of the progress curves indicate that ET is gated by intracomplex conversion among a conformational ensemble.

MATERIALS AND METHODS

The protocols for expression, reconstitution with the desired metalloporphyrin, M (M is Mg-protoporphyrin IX = Mg or Zn-deuteroporphyrin IX = Zn), and purification of Mb(D44K/D60K/E85K) have been outlined elsewhere,[4,5] and are briefly described in the Expanded Materials and Methods section in Supporting Information (SI). The tryptic fragment of bovine cyt b_5 was isolated and purified as described previously.[20,21] Aerobic cyt b_5 prefers the ferric state because of its slight negative redox potential (−0.006 V vs NHE).[22] However, for oxidative quenching experiments in which cyt b_5 served as the oxidizing agent, it was further treated with excess $K_3[Fe(CN)_6]$ and then washed thoroughly with working buffer (5 mM KPi, pH 6). For reductive quenching experiments in which cyt b_5 served as the reducing agent, it was treated with excess $Na_2S_2O_4$ and then washed thoroughly with working buffer.

Samples were prepared in a COY anaerobic glovebox. The working buffer (5 mM KPi, pH 6.0 or 70% w/w glycerol in 5 mM KPi, pH 6) was syringe-filtered and allowed to deoxygenate in the glovebox for at least 24 h before the samples were made. Protein stock solutions were exchanged into the anaerobic working buffer using Corning Spin-X UF concentrators immediately prior to the measurements. Three types of sample were prepared: MMb by itself, cyt b_5 by itself, and the complex, [MMb:cyt b_5]. The details concerning sample volumes and concentrations for femtosecond- and nanosecond-transient absorption (TA) can be found in SI.

Singlet quenching was measured via fs-TA.[23] The ∼120 fs pulses were produced with a commercial Ti:sapphire oscillator/amplifier (Tsunamic/Spitfire, Spectra-Physics), generating ∼1 W at 827 nm, operating at 1 kHz. About 40% of this output was frequency-doubled and directed to a two-stage OPA producing pulses of 540 nm (ZnMb samples) or 598 nm (MgMb samples). Five percent of the amplified pulse was sent up and down a motorized delay track which provided the desired time resolution, then was focused onto a sapphire disk to create a white-light continuum probe with coverage from 430 to 850 nm. After passing through the sample, the probe beam was dispersed onto a CMOS array detector for the collection of spectral data at multiple delay times following photoexcitation of the sample. Samples were stirred to reduce the effects of photodegradation and local heating. Transient absorption spectra were obtained by chopping the pump beam at 500 Hz and subtracting pump-on versus pump-off spectra. Data were treated with a group-delay dispersion correction prior to analysis. Progress curves were generated at multiple wavelengths from the TA spectra and fit using an exponential (for ^{1}MMb decay) or a stretched exponential[24] (for ^{1}MMb reaction with cyt b_5) (see Results and Discussion). Additional experimental and data analysis details are available in SI.

Triplet quenching was measured via ns-TA. Samples were excited with a Nd:YAG Quanta-Ray INDI laser (Spectra-Physics) tuned to 532 nm.[6] The output power was set to approximately 20 mW for the MgMb samples. Triplet measurements were performed with an LKS.60 laser flash photolysis spectrometer (Applied Photophysics) fitted with a xenon lamp with pulsing capabilities as the probe source. The submicrosecond−millisecond collection mode uses an Agilent Infiniium 600 MHz digitizer with a five-stage 1P28 photomultiplier tube as the detector. The xenon lamp was pulsed for submicrosecond collections. The triplet decay time courses were monitored at 465 nm, the maxima for the triplet-ground spectra difference for these samples. All kinetic experiments were performed at 20 °C. As decay traces span several orders of magnitude in time, 50−100 shots were averaged for each time-segment and then merged into single files to obtain full kinetic progress curves for analysis.

RESULTS AND DISCUSSION

Energetics of ET between ^{1}MMb/^{3}MMb and cyt b_5. The driving forces ($-\Delta G^0$) for the charge separation reactions generated by the photoinitiated oxidation or reduction of ^{1}MgMb by ferric cyt b_5 or ferrous cyt b_5, calculated as described in SI, are presented within the ET cycle of Scheme 1 and in Table 1. The driving forces for charge recombination follow

Scheme 1

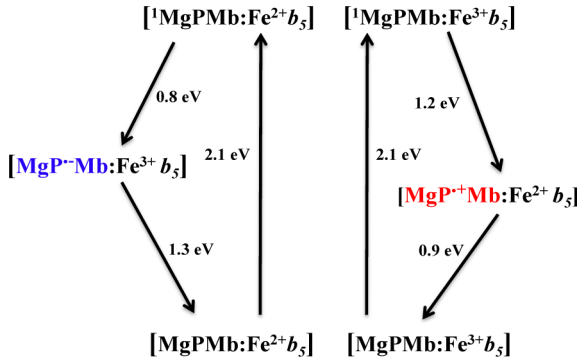

Table 1. Driving Forces ($-\Delta G^0$) for the Singlet and Triplet ET Charge Separation and Recombination Reactions for the [MgMb:Fe^{3+}cyt b_5] and [MgMb:Fe^{2+}cyt b_5] Complexes

		charge separation, $-\Delta G^0$ (eV)	charge recombination, $-\Delta G^0$ (eV)
singlet ET	[^{1}MgMb:Fe^{3+}cyt b_5]	1.2	0.9
	[^{1}MgMb:Fe^{2+}cyt b_5]	0.8	1.3
triplet ET	[^{3}MgMb:Fe^{3+}cyt b_5]	0.8	0.9
	[^{3}MgMb:Fe^{2+}cyt b_5]	0.4	1.3

from closing the thermodynamic cycle and are also given in Scheme 1 and Table 1. Both oxidative *and* reductive ET quenching of ^{1}MgMb by Fe^{3+}cyt b_5 (right side of Scheme 1) and Fe^{2+}cyt b_5 (left side of Scheme 1), respectively, are seen to be strongly energetically favorable ($-\Delta G^0 \gg 0$). The photoinitiated oxidation or reduction charge separation reactions of ^{1}ZnMb by ferric or ferrous cyt b_5 are comparably energetically favorable (Scheme S1 in SI).

The corresponding driving forces ($-\Delta G^0$) for ^{3}MgMb oxidation or reduction charge separation reactions with ferric or ferrous cyt b_5 were calculated analogously; again, both oxidative and reductive ET quenching of ^{3}MgMb by cyt b_5 are highly favorable (Table 1; Scheme S2 in SI).

Singlet State (^{1}MMb) Electron Transfer Quenching. MgMb forms 1:1 cyt b_5 complexes with dissociation constant,

dx.doi.org/10.1021/ja506388c | J. Am. Chem. Soc. 2014, 136, 12730−12736

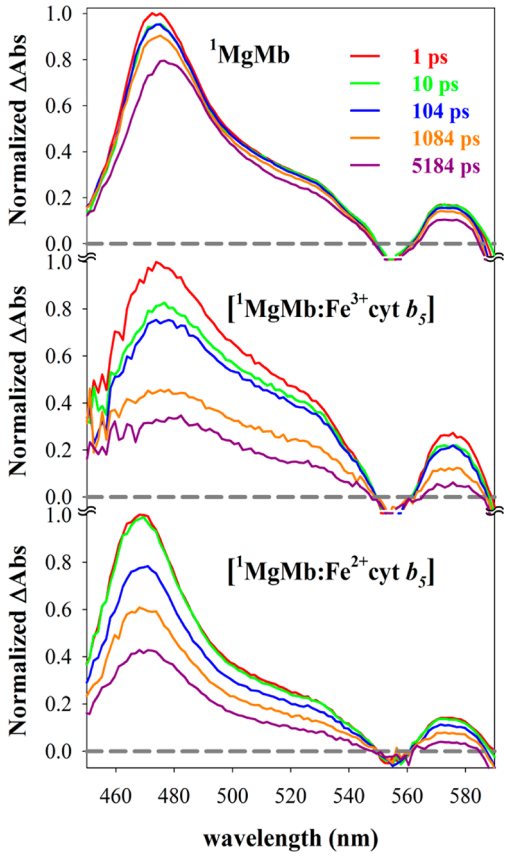

Figure 1. Difference spectra for ^{1}MgMb by itself (top), in complex with Fe^{3+}cyt b_5 (middle), and in complex with Fe^{2+}cyt b_5 (bottom).

$K_d \approx 10\ \mu$M, as does ZnMb.[6] Figure 1 displays the absorbance-difference spectra in the 450−600 nm region, collected subsequent to laser excitation over the time scale of S_1 decay for (i) MgMb by itself (top panel, Figure 1) and for complexes with (ii) Fe^{3+}cyt b_5 (middle, Figure 1) and (iii) Fe^{2+}cyt b_5 (bottom, Figure 1); the concentrations of cyt b_5 were chosen so that ≥ 90% of the MMb was in complex. As can be seen, the singlet-ground absorbance-difference spectra at t = 1 ps for the free MgMb and for the two complexes are essentially the same; the same is true for ZnMb (Figure S1 in SI). The traces of Figure 1 show the ^{1}MgMb difference spectrum collected out to 5.2 ns; the absorbance difference persisting after this time is due to the triplet-ground difference generated by ^{1}MgMb that undergo ISC to ^{3}MgMb, which does not decay on the ns singlet time scale.

As clearly seen in Figure 1, the ^{1}MgMb excited state is strongly quenched by complex formation with the cyt b_5 partner protein in both its Fe^{3+} and Fe^{2+} oxidation states. Analogous behavior is observed for ^{1}ZnMb (Figure S1 in SI), but ^{1}MgMb decays approximately 5 times more slowly than ^{1}ZnMb, allowing for relatively clearer characterization of ^{1}MgMb ET quenching, and consequently, we focus on this variant here. The progress curves for the decay of ^{1}MgMb, both free and in the two complexes were assembled from the absorbance-difference spectra slices at 465 nm and are shown in Figure 2. See Figure S2 in SI for progress curves of free ^{1}ZnMb and in complex with Fe^{3+}cyt b_5 and Fe^{2+}cyt b_5. The free ^{1}MMb (M = Mg, Zn) decays exponentially (eq 1),

$$\Delta A = A_0 \exp(-{}^1k_D t) + C \quad (1)$$

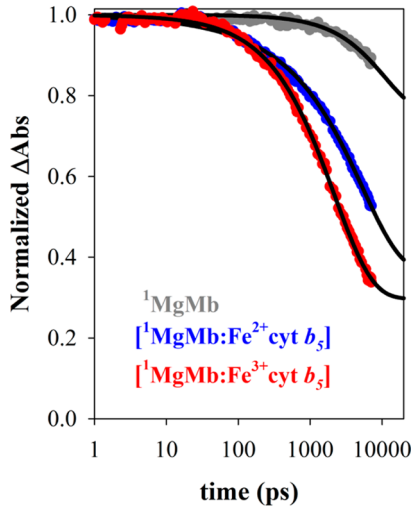

Figure 2. Progress curves for singlet to ground decay for ^{1}MgMb (gray), reductive quenching of ^{1}MgMb in the presence of Fe^{2+}cyt b_5 (blue), and oxidative quenching of ^{1}MgMb in the presence of Fe^{3+}cyt b_5 (red). The ^{1}MgMb trace is described by eq 1, while the [^{1}MgMb:Fe^{2+}cyt b_5] and [^{1}MgMb:Fe^{3+}cyt b_5] traces are best described by eq 2.

where A_0 is the singlet-ground absorbance difference, ^1k_D is the singlet decay constant, and C is the absorbance difference associated with the triplet state, which does not decay measurably on this time scale. Table 2 presents the derived ^1k_D's.

For both the [MMb:Fe^{3+}cyt b_5] and [MMb:Fe^{2+}cyt b_5] complexes, the strong quenching of ^{1}MMb by the cyt b_5 (Figure 1, Figure S1 in SI) generates rapidly decaying progress curves (Figure 2, Figure S2 in SI) that are well described by augmenting the intrinsic decay with a stretched exponential (eq 2).

$$\Delta A = A_0 \exp[-{}^1k_D t - ({}^1k_f t)^n] + C \quad (2)$$

This formulation describes an ensemble of complexes that exhibit a distribution in quenching constants around an average value, ^1k_f, the breadth of the distribution is reflected in the distribution exponent, $0 < n \leq 1$, with smaller values for n corresponding to greater breadth of the distribution.[24]

The quenching constants for both ^{1}MMb's obtained by globally fitting the progress curves of Figures 2 and S2 in SI at multiple wavelengths to eq 2 are presented in Table 2; we note that the quenching constants for ^{1}ZnMb are less reliably obtained because of the more rapid singlet decay. Given the high driving forces for *both* oxidative and reductive ET (Table 1 and Scheme 1) we attribute the S_1 quenching in *both* [^{1}MgMb:cyt b_5] complexes to intracomplex ET: to *photo-oxidation* of the strongly reducing singlet excited state of MgMb through ^{1}MgMb → Fe^{3+}cyt b_5 ET (Scheme 1, right-side of the photocycle) with the rate constant of $^1k_{f,ox}$; to *photoreduction* of the S_1 state by Fe^{2+}cyt b_5 → ^{1}MgMb ET (Scheme 1, left-side of the photocycle) with the rate constant of $^1k_{f,red}$. Likewise, the S_1 quenching in ZnMb complexes is attributed to intracomplex ET due to photooxidation or photoreduction with Fe^{3+}cyt b_5 or Fe^{2+}cyt b_5, respectively (SI). As confirmation, analysis presented in SI demonstrates that resonance energy transfer from the excited ^{1}MgMb/^{1}ZnMb to Fe^{3+} or Fe^{2+}cyt b_5 cannot be a significant component of the quenching.

Efforts to measure the rate constant for charge recombination of the charge separated intermediates generated by ET between ^{1}MgMb/^{1}ZnMb and cyt b_5 were not successful. Such

dx.doi.org/10.1021/ja506388c | J. Am. Chem. Soc. 2014, 136, 12730−12736

Table 2. Fit Parameters for ^{1}MMb (M = Mg, Zn) Decay and Singlet ET with cyt b_5

	[^{1}MgMb:Fe^{2+}cyt b_5]	[^{1}MgMb:Fe^{3+}cyt b_5]	[^{1}ZnMb:Fe^{2+}cyt b_5]	[^{1}ZnMb:Fe^{3+}cyt b_5]
^1k_D (s^{-1})	$9.1(1) \times 10^7$		$4.7(5) \times 10^8$	
^1k_f (s^{-1}), (n)	$2.8(2) \times 10^8$ (n = 0.50)	$3.6(2) \times 10^8$ (n = 0.74)	$2.0(1) \times 10^8$ (n = 0.50)[a]	$2.9(8) \times 10^8$ (n = 0.78)

[a]Due to less cleanly resolved quenching in the ZnMb complexes, the distribution exponent was fixed in eq 2 for [ZnMb:Fe^{2+}cyt b_5] to the value obtained from fits to the [MgMb:Fe^{2+}cyt b_5] progress curves.

measurements were carried out in an earlier study of photooxidation of a more tightly bound ^{1}MMb variant,[6] but that study showed that the charge recombination (back ET) reactions are faster than the charge separation (or forward ET) reactions, suppressing accumulation of the intermediate on the singlet time scale as well as the triplet time scale as discussed below. In the present study, this obstacle was compounded by the fact that in the wavelength range monitored (450−750 nm) there is no singlet/ground isosbestic point that could be used to optimally detect and monitor the intermediate, and the absorbance-difference for the charge-separated species is small relative to the singlet-ground absorbance difference throughout the range.

Surprisingly, the average rate constants for the photooxidation and photoreduction of ^{1}MgMb, respectively within the complexes with Fe^{3+}cyt b_5 and Fe^{2+}cyt b_5, are roughly equal, $^1k_{f,ox} \approx {}^1k_{f,red}$, despite the fact that the driving forces for the two charge separation processes differ by 0.4 eV (Table 1). Likewise, the average photooxidation and photoreduction rate constants of ^{1}ZnMb are also similar (Table 2). In short, the average ET quenching rate constant appears surprisingly insensitive to the direction of the electron flow—being essentially the same when ^{1}MMb is oxidized by Fe^{3+}cyt b_5 or reduced by Fe^{2+}cyt b_5—and ^1k_f is further insensitive to the identity of M (Table 2).

The fits of the ET quenching to a stretched exponential with $n < 1$ imply the presence of an ensemble of complexes with a distribution of singlet ET rate constants. Brownian Dynamics (BD) simulations, indeed predict the presence of such an ensemble, with M−Fe distances that range from 15 to 20 Å and a shortest reactivity distance of 15.3 Å for the complexes between the Mb mutant and cyt b_5.[25] However, the observation of a distribution of quenching constants, rather than an average over the rate constants of the ensemble, further implies that the ensemble of bound complexes do not undergo conformational interconversion on the ET time scale. To test this implication, ET was measured for the [MgMb:Fe^{3+}cyt b_5] and [MgMb:Fe^{2+}cyt b_5] complexes in 70% w/w glycerol buffer, where the viscosity is ∼20× greater than that of aqueous buffer. Figure 3 shows that the singlet kinetic data collected in glycerol and aqueous buffers overlay well for both oxidative and reductive quenching, and ET kinetic parameters for the two solvents differ insignificantly, confirming the absence of any role for conformational interconversion within the ensemble of structures during the nanosecond duration of the singlet ET charge separation process.

Comparison of Oxidative and Reductive Singlet Electron Transfer. We now show that, when the ET energetics for oxidation and reduction charge separation processes (Table 1) are incorporated in the Marcus equation, they fully account for the unexpectedly similar rate constants for the photooxidation and photoreduction of ^{1}MMb within the complexes with Fe^{3+}cyt b_5 and Fe^{2+}cyt b_5, respectively. Marcus showed that an ET rate constant can be written as the product of two terms—the tunneling matrix element (H_{DA}^2) and the Franck−Condon factor (FC). The former is a joint function of

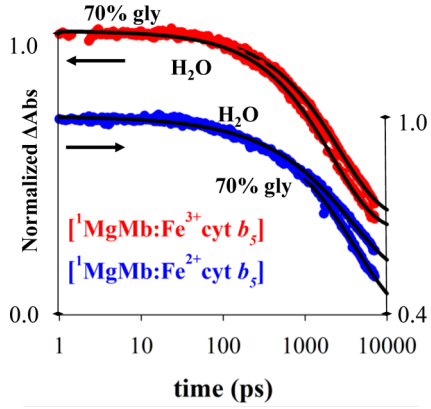

Figure 3. Progress curves for oxidative (red) and reductive (blue, offset by −0.3 arbitrary absorbance units) quenching of ^{1}MgMb by Fe^{3+} and Fe^{2+}cyt b_5, respectively in 70% gly and aqueous buffer.

the distance between the donor and acceptor and the electron-transfer pathways (dictated by the protein as the intervening medium in this case), while the latter is a function of the driving force ($-\Delta G^0$) for the electron transfer reaction, eqs 3,

$$k_{ET} = \frac{2\pi}{\hbar} H_{DA}^2 \cdot FC \tag{3a}$$

$$FC = \frac{1}{\sqrt{4\pi\lambda k_B T}} \exp\left(\frac{-[\Delta G^o + \lambda]^2}{4\lambda k_B T}\right). \tag{3b}$$

FC (eq 3b) is a "simple" parabolic function of the driving force ($-\Delta G^0$) for ET with maximum at $-\Delta G^0 = \lambda$ (where λ is the reorganization energy). Figure 4 plots FC as a function of $-\Delta G^0$ for $\lambda \approx 1$ eV;[25] previous reports have demonstrated that the same λ value is applicable to both oxidative and reductive charge recombination reactions for the same photoexcitable species.[19]

While the [MgMb:Fe^{3+}cyt b_5] and [MgMb:Fe^{2+}cyt b_5] complexes are expected to exhibit a similar ensemble of structures and electron-transfer pathways (due to the same ranges of reactivity distances and the same protein media) and, therefore, comparable H_{DA}^2, the driving forces for the oxidative and reductive ^{1}MgMb ET charge separation processes differ by $\delta(-\Delta G^0) \approx 0.4$ eV (Table 1). However, Figure 4 highlights the unexpected fact that the two driving forces (depicted by circles) are symmetrically placed around and near the maximum of the parabola at $-\Delta G^0 = \lambda$, oxidation being in the "inverted" region, $-\Delta G^0 > \lambda$, reduction in the "normal" region, $-\Delta G^0 < \lambda$. As a result, FC for the two processes is fortuitously the same. Moreover, since the two driving force values fall near the FC maximum, slight adjustments of either the $-\Delta G^0$'s or λ would likely result in the same set of kinetic observations. Thus, the apparently surprising similarities in the ^1k_f for the oxidative and reductive quenching of ^{1}MgMb are understandable on simple energetic grounds.

dx.doi.org/10.1021/ja506388c | J. Am. Chem. Soc. 2014, 136, 12730−12736

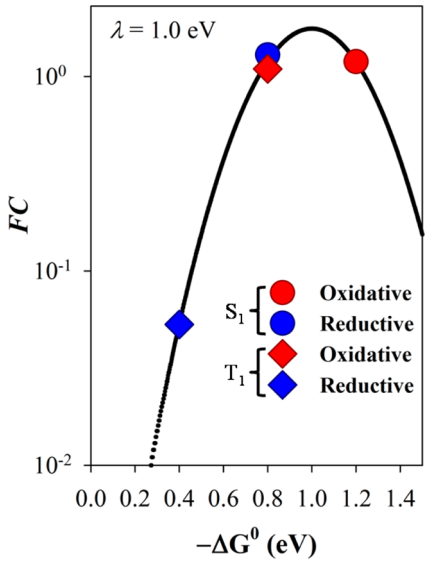

Figure 4. *FC* term as a function of driving forces ($-\Delta G^0$) and λ = 1.0 eV for ET in the MgMb complexes with cyt b_5. Singlet ET is represented by circles, and triplet ET, by diamonds. Oxidative quenching or ET from ^{1,3}MgMb to Fe^{3+}cyt b_5 is in red and reductive quenching or ET from Fe^{2+}cyt b_5 to ^{1,3}MgMb is in blue. Since $-\Delta G^0$ = 0.8 eV (see Table 1) for reductive quenching due to singlet ET and oxidative quenching due to triplet ET, the *FC* terms for these two processes are offset by 0.1 in opposite directions for clarity.

Likewise, $-\Delta G^0$'s for singlet ET charge separation processes in the [^{1}ZnMb:Fe^{3+}cyt b_5] and [^{1}ZnMb:Fe^{2+}cyt b_5] complexes are symmetrically related to λ (Figure S4 in SI), again explaining why the oxidative and reductive singlet ET quenching reactions have similar ^1k_f's (Table 2). Additionally, the respective oxidative and reductive ET charge separation processes for the [^{1}ZnMb:cyt b_5] complexes have driving forces that are within $\delta(-\Delta G^0) \approx 0.1$ eV (Scheme S1 in SI) of those for the [^{1}MgMb:cyt b_5] complexes (Scheme 1; Table 1), accounting for the M-independence of ET rate constants.

Examination of the parameter characterizing the breadth of the distribution in structures (n, eq 2) does, however, reveal a slight oversimplification in the above comments about H_{DA}^2. For both M = Mg and Zn, the distribution parameter for oxidative singlet ET quenching ($n \approx 0.75$) appears to be meaningfully different than that for reductive singlet ET quenching ($n \approx 0.50$) suggesting a broadening of the distribution of rate constants for reductive quenching in the complex, [^{1}MgMb:Fe^{2+}cyt b_5], relative to oxidative quenching in the complex, [^{1}MgMb:Fe^{3+}cyt b_5] (Table 2). This dissimilarity can be attributed to a subtle variance in the ensemble of binding geometries resulting from the difference by a single charge in the two oxidation states, ferrous and ferric, of the highly negative cyt b_5 partner in the two types of complexes.

Oxidative and Reductive Electron Transfer in [^{3}MgMb:cyt b_5] Complexes. Conformations of the [^{1}MgMb:cyt b_5] complexes that do not react via singlet ET (or relax to ground) instead undergo ISC to the [^{3}MgMb:cyt b_5] state, which can react via photooxidation or photoreduction of ^{3}MgMb by the Fe^{3+}cyt b_5 and Fe^{2+}cyt b_5, respectively, on the much longer (ms) triplet-state time scale. Figure 5 presents progress curves for triplet decay monitored at 465 nm, the maximum triplet-ground difference absorption wavelength, for samples of the [MgMb:Fe^{3+}cyt b_5] complex and the [MgMb:Fe^{2+}cyt b_5] complex in aqueous and 70% w/w glycerol buffers; in both cases ~80% of the MgMb was in complex.

In the absence of cyt b_5, ^{3}MgMb decays to the ground state with first-order rate constant, ^3k_D = 400 s^{-1} independent of solvent (Figure 5). As previously reported, the [Mb:cyt b_5] complex is in the slow-exchange regime on the triplet ET time scale where ET is significantly faster than dissociation of the

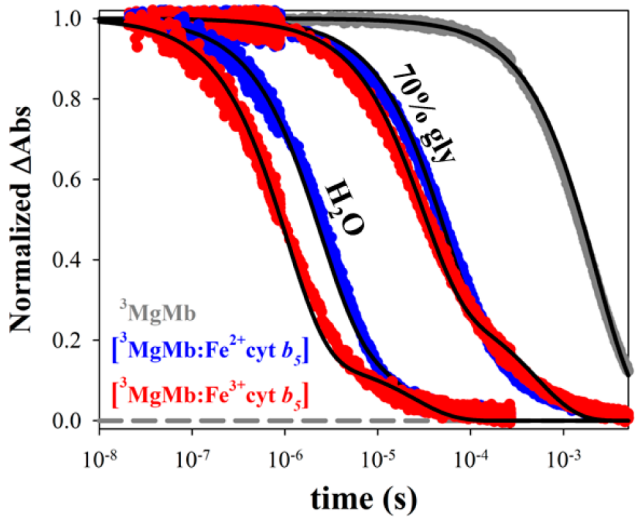

Figure 5. Triplet progress curves monitored at 465 nm: MgMb by itself in the absence of cyt b_5 quencher in gray; in the presence of Fe^{2+}cyt b_5 in blue; in the presence of Fe^{3+}cyt b_5 in red. Triple ET slows down with increased viscosity as noted by the rightward shift (toward ^3k_D) of the progress curves in 70% gly relative to the ones in aqueous buffer.

complex, $^3k_{ET} \gg k_{off}$.[6] As a result, triplet decay traces for the complex are biphasic (Figure 5) and can be fit to a double exponential (eqs 4): the rapidly decaying majority phase corresponds to the [^{3}MgMb:cyt b_5] complex (fraction R), which decays with rate constant, $^3k_{obs,f} = {}^3k_D + {}^3k_f$ where ^3k_f is the intracomplex triplet ET rate constant; the minority phase represents free ^{3}MgMb, which undergoes slower bimolecular quenching ($^3k_2$) with pseudo-first-order rate constant $^3k_{obs,s} = {}^3k_D + {}^3k_2$*[cyt b_5].

$$\Delta A = A_0[R^*\exp(-{}^3k_{obs,f}t) + (1 - R)^*\exp(-{}^3k_{obs,s}t)] \quad (4a)$$

where

$${}^3k_{obs,f} = {}^3k_D + {}^3k_f;\ {}^3k_{obs,s} = {}^3k_D + {}^3k_2^*[\text{cyt } b_5] \quad (4b)$$

The kinetic parameters resulting from fits to eqs 4 are listed in Table 3. Monitoring the triplet/ground isosbestic points yielded no quantifiable charge-separated intermediate signals for either the oxidative or reductive quenching charge separation triplet ET reactions, supporting the expectation that the accumulations of the respective charge-separated species are even smaller on the triplet time scale relative to the singlet time scale due to the relative lifetimes of the charge separation and charge recombination processes.[26]

The rate constants for intracomplex triplet ET, ^3k_f's, are essentially the same for the oxidative and reductive processes in the same type of solvent (Table 3), but in this case the identity is not in agreement with predictions of the Marcus theory based on the energetics for triplet ET quenching. As with

dx.doi.org/10.1021/ja506388c | J. Am. Chem. Soc. 2014, 136, 12730−12736

Table 3. ^3k_f's (s^{-1}) and $^3k_2$'s (mM^{-1} s^{-1}) for ^{3}MgMb Reductive and Oxidative Quenching in Water and 70% w/w Glycerol

	^3k_f (s^{-1}), R		$^3k_2$ (mM^{-1} s^{-1})	
	water, 1.005 cP (20 °C)	70% w/w gly, 22.5 cP (20 °C)	water, 1.005 cP (20 °C)	70% w/w gly, 22.5 cP (20 °C)
[^{3}MgMb:Fe^{3+}cyt b_5]	9.7(1) × 10^5, 0.85	3.3(5) × 10^4, 0.71	8.1(2) × 10^5	3.1(6) × 10^4
[^{3}MgMb:Fe^{2+}cyt b_5]	4.3(6) × 10^5, 0.77	1.9(3) × 10^4, 0.79	1.1(2) × 10^6	2.4(4) × 10^4

singlet ET, triplet ET is energetically favorable for both oxidative quenching ($-\Delta G^0$ = 0.8 eV) and reductive quenching ($-\Delta G^0$ = 0.4 eV) of the ^{3}MgMb with the difference between these two driving forces also being ∼0.4 eV (Table 1). At the same time, the relative driving forces ($-\Delta G^0$) are not symmetrically positioned around the estimated λ (Figure 4), and the *FC*, and $^3k_{ET}$ is predicted to differ by more than an order of magnitude for the two charge separation processes: $^3k_{ET,ox} > {}^3k_{ET,red}$.

The similarity of the two ^3k_f's instead are explained by comparing the progress curves for the complexes in aqueous ($\eta \approx 1$) and 70% w/w glycerol buffers ($\eta \approx 20$). As expected, the diffusion-limited second-order process slows in 70% w/w gly relative to water for both the photooxidative and photoreductive reactions with $^3k_2$ decreasing by a factor of $\gtrsim 20$ as the viscosity increases by about this factor (Table 3). Unexpectedly, the rate constants for both oxidative and reductive intracomplex ET decrease by roughly the same factor (Table 3). This equality and viscosity-dependence of the rate constants for intracomplex oxidative and reductive triplet ET, $^3k_{f,ox} \approx {}^3k_{f,red}$, demonstrates that the measured intracomplex rate constant for charge separation reflects not the ET process itself but rather the rate constant for interconversion among conformations of the bound complex; conformational interconversion on the μs−ms time scale serves as a "gate" to the intracomplex charge separation triplet ET.[27,28]

SUMMARY

We have shown that photoinitiated electron flow within the [MMb:cyt b_5] complex (M = Mg or Zn) that is stabilized by three D/E → K mutations of Mb can indeed be "symmetrized"; the complex exhibits both oxidative *and* reductive ET quenching of both the singlet *and* triplet photoexcited MMb states, with the direction of electron flow being determined by the oxidation state of the cyt b_5 partner, Fe^{3+}cyt b_5 or Fe^{2+}cyt b_5. Despite a large disparity in driving force in favor of photooxidation relative to photoreduction ($\delta(-\Delta G^0) \approx 0.4$ eV, M = Mg; ≈ 0.2 eV, M = Zn), the ultrafast intracomplex reductive and oxidative ET quenchings of ^{1}MMb surprisingly have the same average ET rate constants of $^1k_f \approx 10^8$ s^{-1}. Equally surprising, the intracomplex reductive and oxidative ET quenchings of ^{3}MMb are again the same within error, $^3k_f \approx 10^5$ s^{-1}.

The equality of the rate constants for photooxidation and photoreduction of ^{1}MMb is explainable on energetic grounds; the driving forces for the two reactions have values symmetrically displaced above and below that of the reorganization energy, λ, and thus equal Franck−Condon factors (*FC*) within the Marcus equation. The progress curves for both directions of electron flow during ET quenching of ^{1}MMb are nonexponential and viscosity independent, implying the presence of an ensemble of structures that do not interconvert on the time scale of the measurement.

The rate constants for photooxidation and photoreduction of ^{3}MMb are again equal despite a large difference in driving force, but in this case the driving force difference predicts a large difference in *FC* and thus in rate constant. This behavior is explained by the findings that the progress curves are exponential and the rate constants decrease inversely with viscosity, which indicate that the quenching constants are not ET rate constants at all, but instead that the reactions are gated by intracomplex conformational interconversion. The control of ET on the time scale of triplet-state quenching by conformational interconversion underscores the important point that protein motions can control even intracomplex ET reactions when they occur on the μs−ms time scale, suggesting that reconsideration of numerous such earlier studies might be productive, whereas the independence of the singlet-state ET from such motions indicates that they are not likely to affect the relatively few ET reactions on the ns time scale.

ASSOCIATED CONTENT

Supporting Information

Expanded Materials and Methods, determination of driving forces for singlet and triplet electron transfer, difference spectra and kinetic traces for [^{1}ZnMb:cyt b_5], Förster resonance energy transfer considerations, and Marcus plot for [^{1}ZnMb:cyt b_5] complexes. This material is available free of charge via the Internet at http://pubs.acs.org.

AUTHOR INFORMATION

Corresponding Author

bmh@northwestern.edu

Notes

The authors declare no competing financial interest.

ACKNOWLEDGMENTS

N.P.C. and B.M.H. gratefully acknowledge financial support from the National Institute of Health (HL 63203). This work was also supported by the Chemical Sciences, Geosciences, and Biosciences Division, Office of Basic Energy Sciences, DOE under Grant No. DE-FG02-99ER14999 (M.R.W.). R.M.Y. gratefully acknowledges the Camille and Henry Dreyfus Postdoctoral Program in Environmental Chemistry for support. R.M.Y and A.L.S. were supported as part of the ANSER Center, an Energy Frontier Research Center funded by the U.S. Department of Energy, Office of Science, Office of Basic Energy Sciences, under Award Number DE-SC0001059.

REFERENCES

(1) Hickson, R. C.; Rosenkoetter, M. A. *Am. J. Physiol.* **1981**, *241*, C140.
(2) Hagler, L.; Coppes, R. I., Jr.; Herman, R. H. *J. Biol. Chem.* **1979**, *254*, 6505.
(3) Liang, Z.-X.; Jiang, M.; Ning, Q.; Hoffman, B. M. *JBIC* **2002**, *7*, 580.
(4) Trana, E. N.; Nocek, J. M.; Knutson, A. K.; Hoffman, B. M. *Biochemistry* **2012**, *51*, 8542.
(5) Nocek, J. M.; Knutson, A. K.; Xiong, P.; Co, N. P.; Hoffman, B. M. *J. Am. Chem. Soc.* **2010**, *132*, 6165.
(6) Xiong, P.; Nocek, J. M.; Vura-Weis, J.; Lockard, J. V.; Wasielewski, M. R.; Hoffman, B. M. *Science* **2010**, *330*, 1075.
(7) Conklin, K. T.; McLendon, G. *Inorg. Chem.* **1986**, *25*, 4804.

(8) Cheng, J.; Zhou, J. S.; Kostic, N. M. *Inorg. Chem.* **1994**, *33*, 1600.
(9) Low, D. W.; Winkler, J. R.; Gray, H. B. *J. Am. Chem. Soc.* **1996**, *118*, 117.
(10) Hoffman, B. M.; Celis, L. M.; Cull, D. A.; Patel, A. D.; Seifert, J. L.; Wheeler, K. E.; Wang, J.; Yao, J.; Kurnikov, I. V.; Nocek, J. *Proc. Natl. Acad. Sci. U.S.A.* **2005**, *102*, 3564.
(11) Magner, E.; McLendon, G. *J. Phys. Chem.* **1989**, *93*, 7130.
(12) Zhou, J. S.; Tran, S. T.; McLendon, G.; Hoffman, B. M. *J. Am. Chem. Soc.* **1997**, *119*, 269.
(13) Zang, L.-H.; Maki, A. H. *J. Am. Chem. Soc.* **1990**, *112*, 4346.
(14) Berglund, J.; Pascher, T.; Winkler, J. R.; Gray, H. B. *J. Am. Chem. Soc.* **1997**, *119*, 2464.
(15) McLendon, G. L.; Winkler, J. R.; Nocera, D. G.; Mauk, M. R.; Mauk, A. G.; Gray, H. B. *J. Am. Chem. Soc.* **1985**, *107*, 739.
(16) Chibisov, A. K. *Photochem. Photobiol.* **1969**, *10*, 331.
(17) Carapellucci, P. A.; Mauzerall, D. *Ann. N.Y. Acad. Sci.* **1975**, *244*, 214.
(18) Shen, C. Y.; Kostic, N. M. *Inorg. Chem.* **1996**, *35*, 2780.
(19) Jankowska, K. I.; Pagba, C. V.; Chekler, E. L. P.; Deshayes, K.; Piotrowiak, P. *J. Am. Chem. Soc.* **2010**, *132*, 16423.
(20) Lloyd, E.; Ferrer, J. C.; Funk, W. D.; Mauk, M. R.; Mauk, A. G. *Biochemistry* **1994**, *33*, 11432.
(21) Funk, W. D.; Lo, T. P.; Mauk, M. R.; Brayer, G. D.; MacGillivray, R. T. A.; Mauk, A. G. *Biochemistry* **1990**, *29*, 5500.
(22) Wang, Y.-H.; Cui, J.; Sun, Y.-L.; Yao, P.; Zhuang, J.-H.; Xie, Y.; Huang, Z.-X. *J. Electroanal. Chem.* **1997**, *428*, 39.
(23) Young, R. M.; Dyar, S. M.; Barnes, J. C.; Juricek, M.; Stoddart, J. F.; Co, D. T.; Wasielewski, M. R. *J. Phys. Chem. A* **2013**, *117*, 12438.
(24) Berberan-Santos, M. N.; Bodunov, E. N.; Valeur, B. *Chem. Phys.* **2005**, *315*, 171.
(25) Keinan, S.; Nocek, J. M.; Hoffman, B. M.; Beratan, D. N. *Phys. Chem. Chem. Phys.* **2012**, *14*, 13881.
(26) Given that the driving forces ($-\Delta G_0$) and consequently the expected ET rate constants for the two back reactions (charge recombination) are the same on both the singlet and triplet timescales (Table 1), the accumulations of the charge-separated species are expected to be even smaller on the triplet time scale than on the singlet time scale as the charge recombination processes are expected to be much faster than the preceding triplet ET charge separation processes based on the relative driving forces.
(27) Hoffman, B. M.; Ratner, M. R. *J. Am. Chem. Soc.* **1987**, *109*, 6237.
(28) Patel, A. D.; Nocek, J. M.; Hoffman, B. M. *J. Phys. Chem. B* **2008**, *112*, 11827.